Noise studies with Crab Cavities in the SPS for the HL-LHC project

UNIVERSITY OF LIVERPOOL

Thesis submitted in accordance with the requirements of the University of Liverpool for the degree of Doctor in Philosophy

by

Natalia Triantafyllou

Day Month Year

Abstract

Acknowledgments

List of Figures

List of Tables

List of Symbols

E_b	Energy
CC	Crab Cavity
V_{CC}	CC voltage
f_{CC}	*CC* frequency
ϕ_{CC}	*CC* phase
$\mathrm{Q_x}$	Horizontal tune
$\mathrm{Q_y}$	Vertical tune
ψ_{y}	Vetical phase advance

Contents

Chapter 1

Introduction

This is the introduction of my PhD thesis.

Testing for footers and headers Testing citation [1]. wefefklje

Test list of symbols with E_b .

Chapter 2

Basics of accelerator beam dynamics

Chapter 3

Theory of Crab Cavity noise induced emittance growth

Chapter 4

First experimental studies with Crab Cavities in the SPS

In 2018, two prototype Crab Cavities (CCs) were installed in the SPS to be tested for the first time with proton beams. A series of dedicated machine developemnt studies was carried out in order to validate their working principle and answer various beam dynamic questions. This chapter provides a comprehesive insight into the operational setup, the applied measurement methods and some of the first experimental with CCs in the SPS. These methods and procedures were developed at CERN and they are presented here as they are essential for the understadning of the work discussed in the following chapters.

The chapter is stractured as follows: Section 4.1 describes the installation of the CCs in the SPS and the experimental machine configuration. The use of the Head-Tail (HT) monitor as the main diagnostic device for measurement of the crabbing is presented in Section 4.2. Last, the analysis of the HT measurements for the callibration of the CC voltage and the reconstruction of the crabbing are discussed in Sections .. and .. respectively.

4.1 Crab Cavities in the SPS

For the SPS tests two prototype CCs of the Double Quorter Wave (DQW) type were fabricated by CERN and were assembled into the same cryomodule which is shown in Fig. 4.1 [2]. The cryomodule was installed in the SPS-LSS6 zone, Fig. 4.2, and was placed on a mobile transfer table [3]. The table moved with high precision and without breaking the vaccum the cryomodule in the beam line for the CC tests and out of it for the usual SPS operation. The main parameters for the CC experiments in SPS are shown in Table 4.1

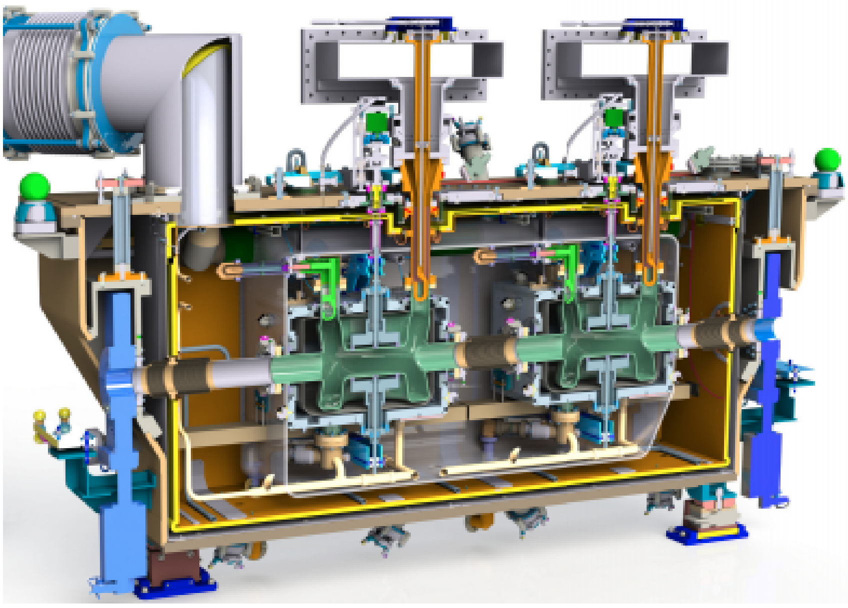

Figure 4.1: Cut of the CC cryomodule [2].

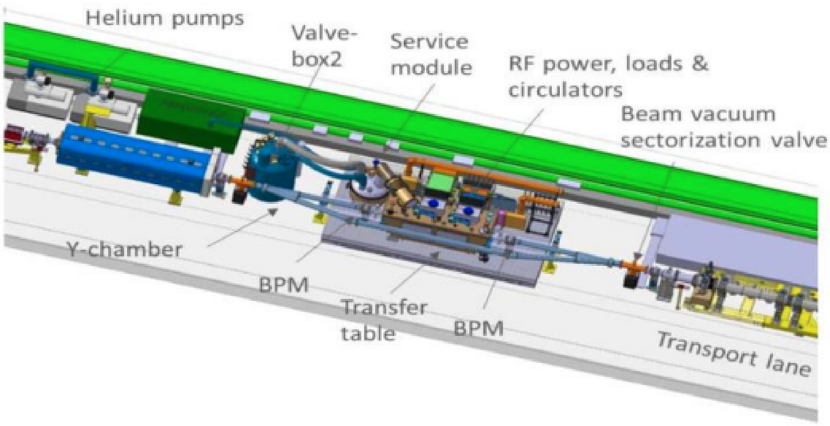

Figure 4.2: Installation of the cryomodule in the SPS-LSS6 zone [3].

Table 4.1: Parametes for the SPS CC tests

Parameters	**Units**	**Values**	
E_b	[GeV]	26, 270	
Main RF frequency	[MHz]	200	
Q_x / Q_y	[-]	26.13 / 26.18	
		CC1	**CC2**
crabbing plane	[-]	vertical	vertical
s-location	[m]	6312.72	6313.32
V_{CC}, MAX	[MV]	4.3	4.3
f_{CC}	[MHz]	400	400
$\beta_{x,CC}$ / $\beta_{y,CC}$	[m]	29.24 / 76.07	30.31 / 73.82
$\alpha_{x,CC}$ / $\alpha_{y,CC}$	[m]	-0.88 / 1.9	-0.91 / 1.86
$D_{x,CC}$ / $D_{y,CC}$	[m]	-0.48 / 0	-0.5 / 0

4.1.1 Operational considerations

For the beam tests with the CCs in the SPS the approach regarding the energy ramp and the adjustment of the phasing with the main RF system needed to be evaluated and they are briefly discussed here.

Energy ramp

SPS recieves the beam at 26 GeV. It was observed that if the ramp to higher energies was performed with the CC on, the beam was lost while crossing one of the vertical betatron sidebands due to resonant excitation [4]. Therefore, it was established the energy ramp has to be performed with the CC off and its voltage must be set up only after the energy of interest has been achieved. It should be noted here that this will be the approach also for the HL-LHC.

Crab Cavity - main RF synchronisation

Another issue of concern was the fact that the CC operate at the fixed frequency of 400 MHz while the SPS main RF system operates at 200 MHz. In order to make sure that the beam will experience the same effect from the CC each turn the SPS main RF has to be re-phased such as it becomes synchronous with the crabbing signal.

For studies at the injection energy of 26 GeV this synchronisation took place shortly after the injection. For studies at 270 GeV, like the emittance growth measurements, the synchronisation took place at the end of the ramp shortly after the cavity was switched on.

4.2 Diagnostics: The Head-Tail monitor

The HT monitor was the main diagnostic device in the SPS CC tests. It was deployed for the measurement of the crabbing and the callibration of the CC voltage. In the first part of this section some general information on the instrument along with example signals will be presented. Subsequently, the post processing of the HT signal in the presence of the CCs will be discussed and then the callibration of the monitor will also be briefly explained. Last, the measurement of the CC voltage and the reconstuction of the crabbing will be presented. The experiemental data presented in this section were acquired at the SPS injection energy of 26 GeV with only one CC, CC1, at ϕ_{CC} for simplicity. This energy option was chosen as the effect of CC kick is stronger and thus more visible than in higher energies.

The Heat-Tail monitor

A standard beam position monitor (BPM) measures the bunch centroid position in

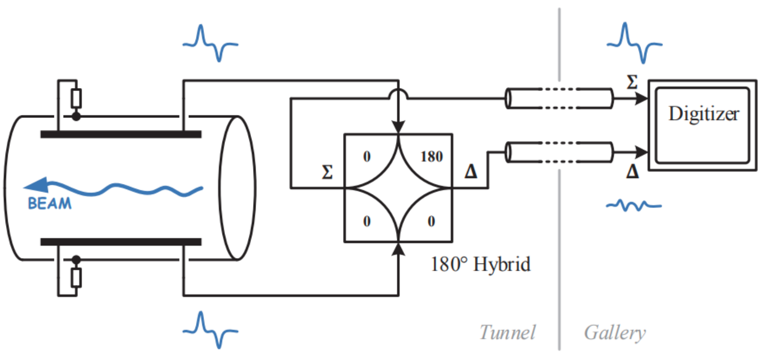

Figure 4.3: Diagram of the SPS HT monitor [5].

the transverse planes at every passage of the beam. The HT monitor is a high bandwidth version of a standard BPM and can measure the transverse offset within the bunch, which makes it ideal for the measurement of the crabbing. Its reading consists of the sum Σ and the difference Δ of the electrode signals of a straight stripline coupler (Fig. 4.3) [6, 5]. The Σ signal is the longitudinal line density while the Δ signal corresponds to the intra-bunch offset. Example signlas obtained from the HT monitor are displayed in Fig. 4.4- 4.6.

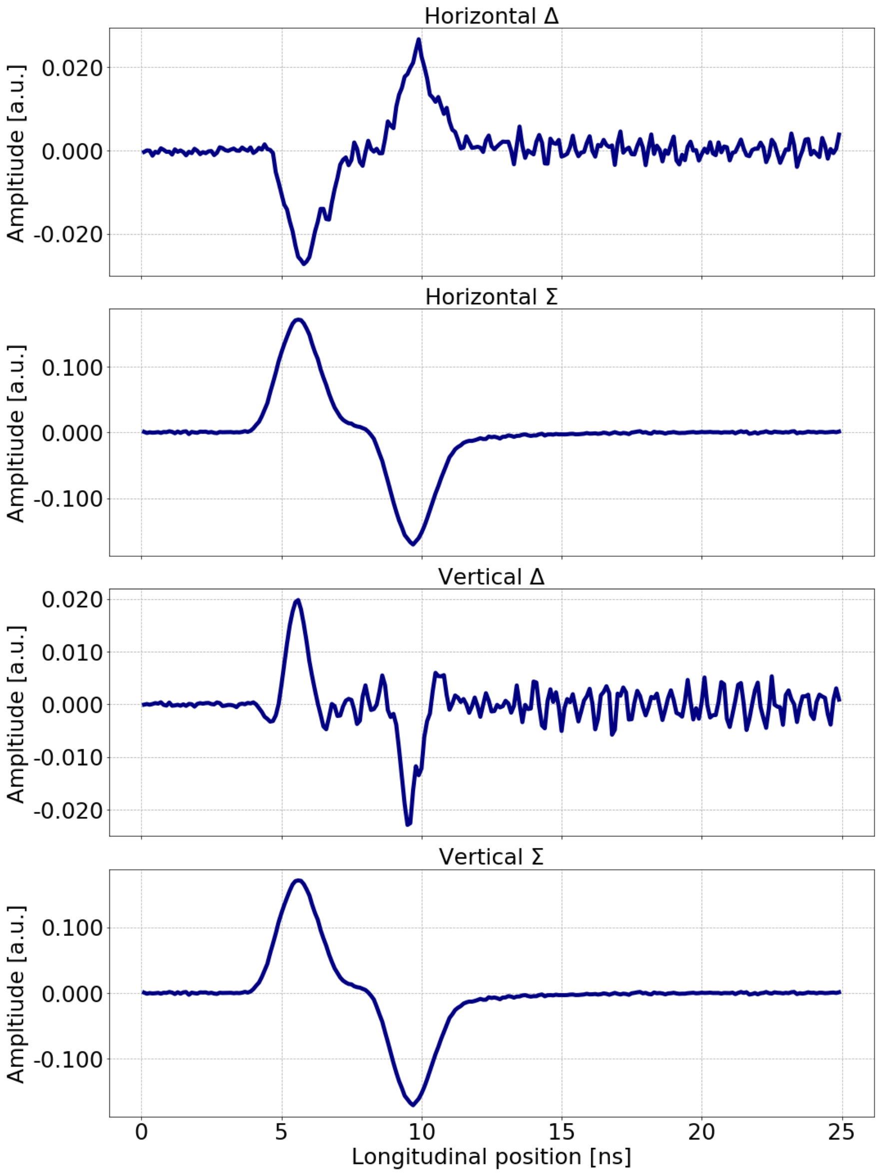

Figure 4.4: Raw example Δ and Σ signals obtained from the HT monitor for a window of 25 ns, acquired in a single SPS revolution.

In particular, Fig. 4.4 and Fig. 4.5 illustrate the signal acquired over a single and multiple turns of the bunch around SPS respectively. The part of the signal after ∼ 9 ns is just the reflected pulse of the bunch signal from the opposite end of the stripline. Moreover, Fig. 4.6 shows a 2D representation of the HT monitor reading. It is worth

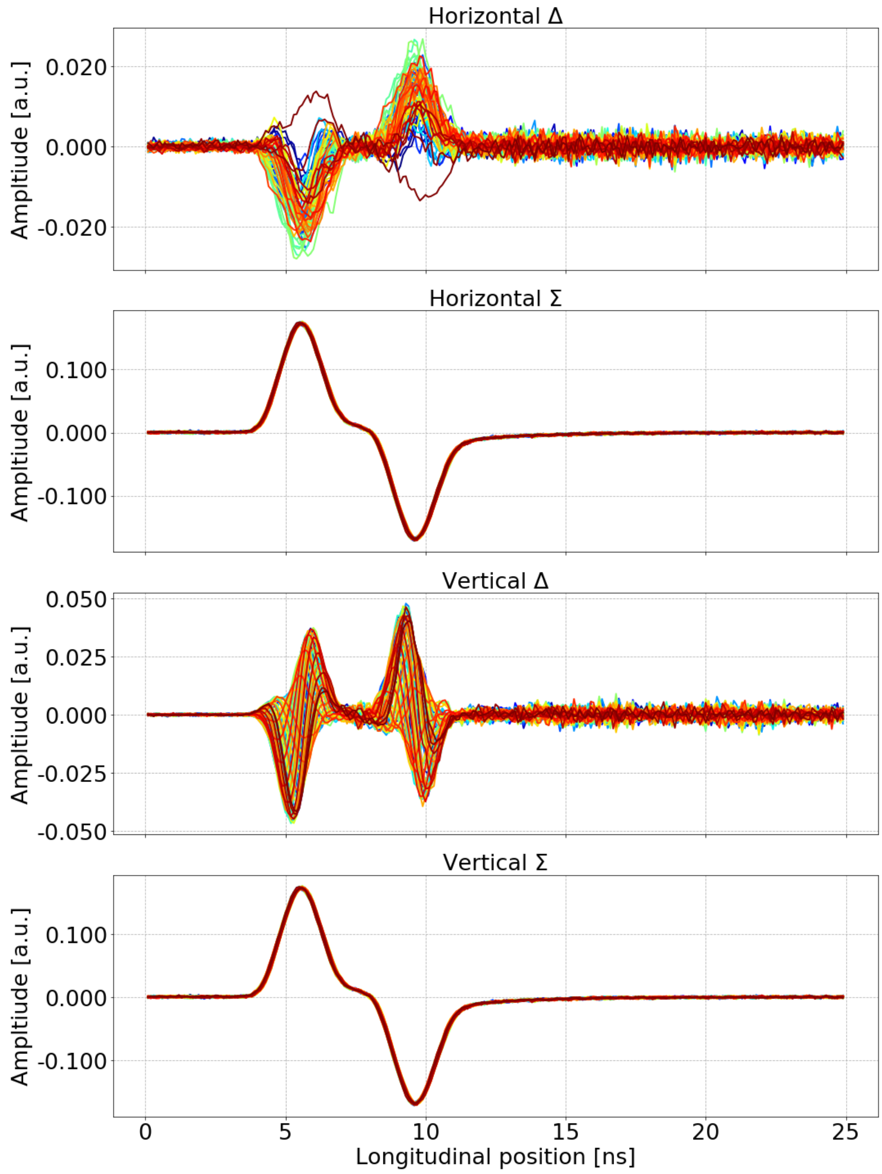

Figure 4.5: Example Δ and Σ signals obtained from the HT monitor for a window of 25 ns, acquired over several SPS revolutions. The color code indicates the different turns around the machine.

mentioning already that in the specific example a clear periodic oscillation of the vertical intra-bunch offset (vertical Δ) signal is observed. This is a result of the main RF system not being synchronous with the CC frequency.

Heat-Tail monitor baseline removal

One issue of concern at that point was the correction of the Δ signal baseline due to orbit offsets and non-linearities of the instrument [5]. Normally, the baseline is removed by computing the mean of the Δ signals over all turns and then subtract-

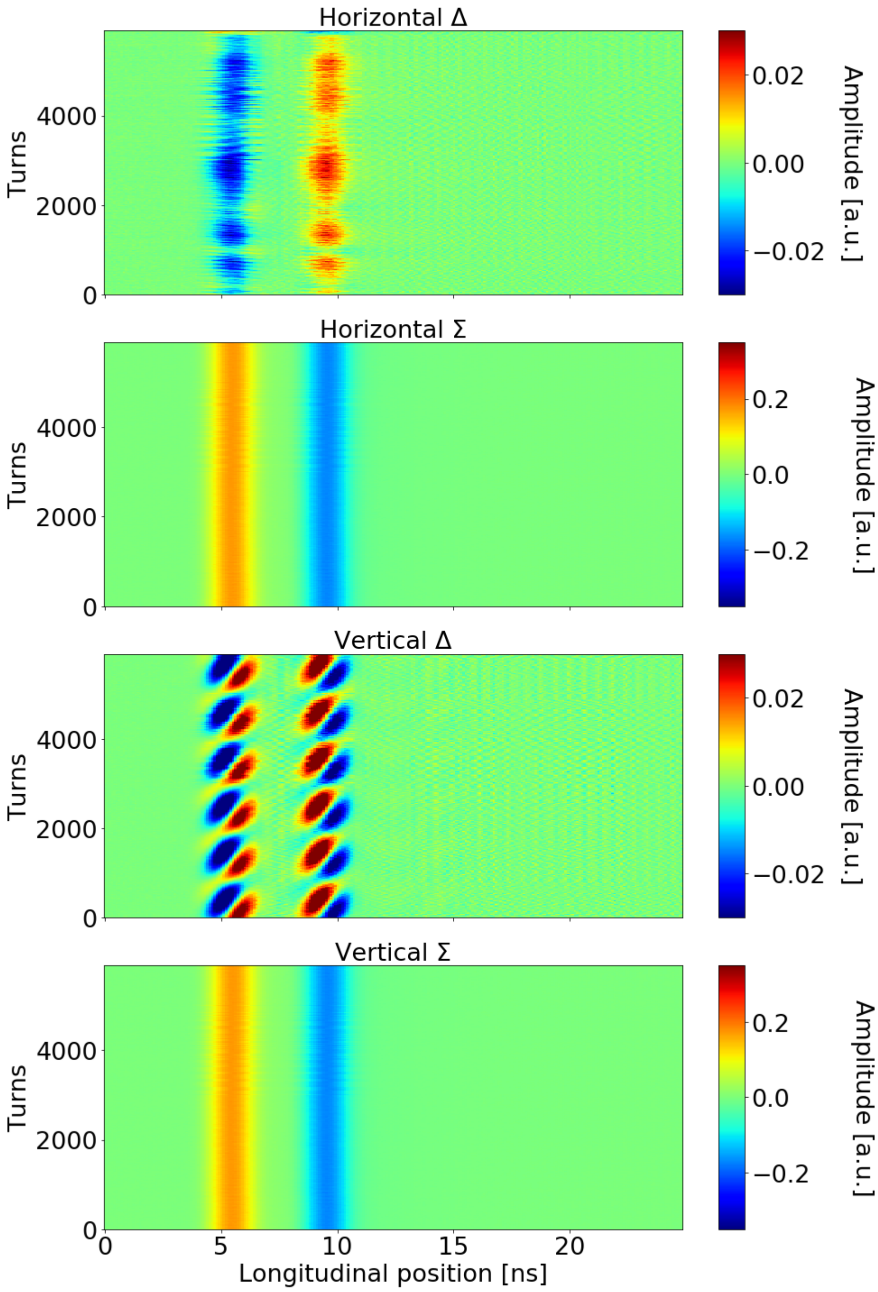

Figure 4.6: 2D representation of example Δ and Σ signals obtained from the HT monitor for a window of 25 ns, acquired over several SPS revolutions.

ing this mean from the signal of each turn. However, in the presence of the CCs this method would also remove the crabbing signal, the static intra-bunch position offset induced by the CC kick when the latter is well synchronised with the main RF system (Section 4.1)).

Therefore, in the SPS experiments a reference measurement had first to be made with the CC unsynchronised. The mean of the Δ signal over this reference period was the baseline which then was subtracted from the Δ signals acquired after the synchronisation (Fig 4.7). The datasets before and after synchronisation are easily detectable in the 2D HT monitor reading as displayed in Fig. 4.8

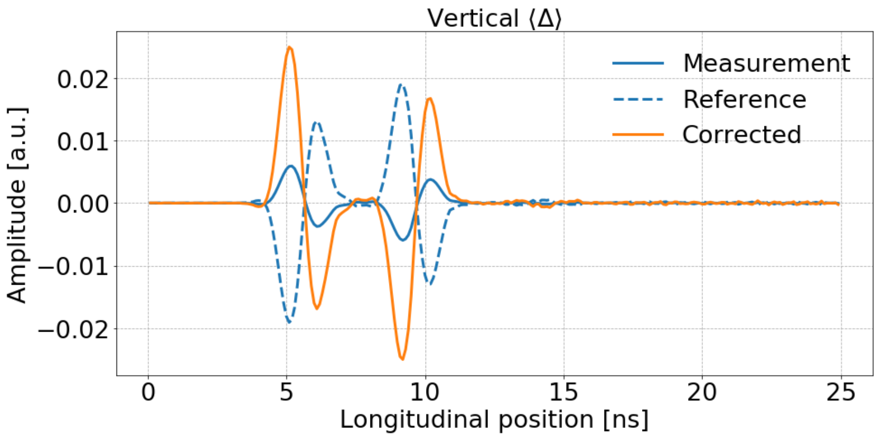

Figure 4.7: HT monitor baseline correction for the SPS CC tests.

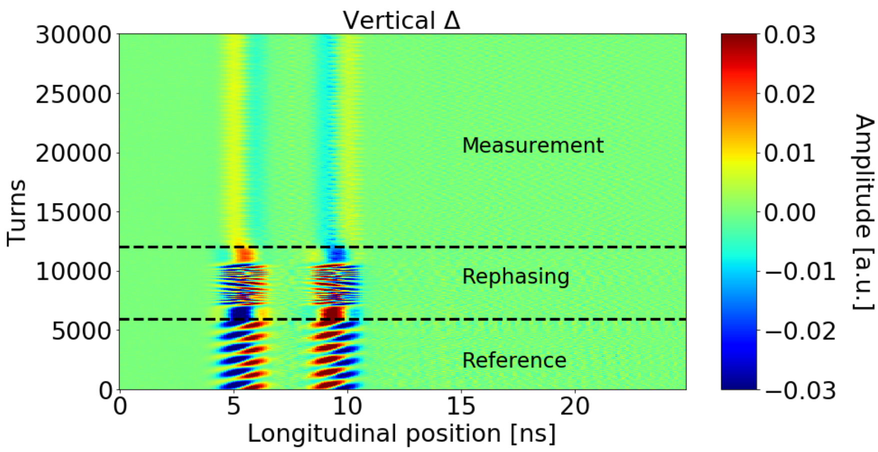

Figure 4.8: HT acquistions before and after the sunchronisation of the SPS main RF with the CC.

Headtail monitor callibration

In order to have the mean intra-bunch offset (Δ) signal in units of mm the Δ acquisitions need to be divided by the Σ signal and by a normalisation factor which is provided by the callibration of the HT monitor [7]. The normalisation factor for the SPS was measured at 0.1052 in 2017. Figure 4.9 shows the intra bunch offset from the CC kick in mm and after the baseline correction. The reflected part of the signal is discarded here and only the crabbing is shown.

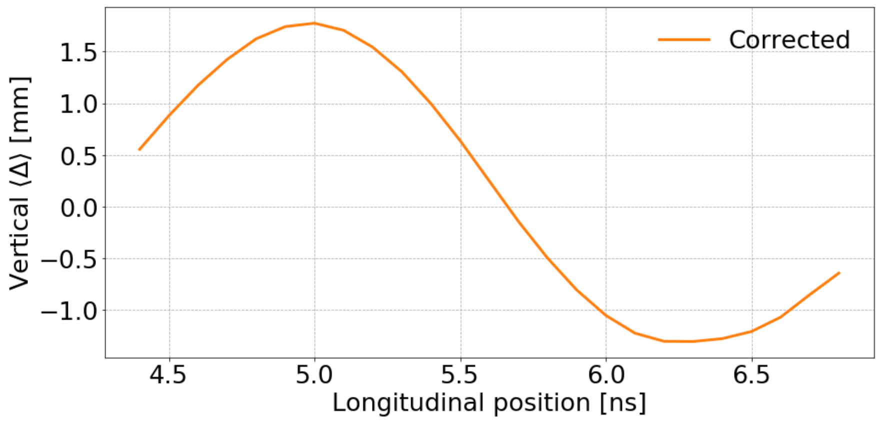

Figure 4.9: Intra-bunch offset from the CC kick expressed in mm after the removal of the baseline.

4.3 Crab Cavity voltage calibration

This section discusses the beam based measurement of the CC voltage from the HT monitor measurements. The calibration was performed by calculating the kick required to reconstruct the measured intra-bunch offset using Eq. (4.1). Equation (4.1), which is obtained from Chaos' Eq... in Ref. [8], gives the vertical orbit shift (in meters) from the CC kick, θ, at the HT monitor location as follows:

$$\Delta y_{,HT} = \frac{\sqrt{\beta_{y,HT}}}{2\sin(\pi \mathrm{Q_y})}\theta\sqrt{\beta_{y,CC}}\cos(\pi \mathrm{Q_y} - \mid \psi_{y,HT} - \psi_{y,CC} \mid), \tag{4.1}$$

where β_y is the beta function, $\mathrm{Q_y}$ is the tune, and ψ_y is the phase advance in tune units. The same applies for the horizontal plane. The indeces HT and CC indicate the optic parameters at the location of the HT monitor and CC respectively.

The deflection from the CC is written as $\theta = -\frac{qV(t)}{E_b}$, where q is the charge of the particle, E_b the beam energy and $V_{CC}(t) = V_{CC}\sin(2\pi f_{CC}t + \phi_{CC})$ is the voltage that a particle experiences while passing through the CC. Computing the maximum of $V_{CC}(t)$ gives the cavity voltage, V_{CC}.

It should be noted here, that the measured intra-bunch offset, $\Delta y_{,HT}$, is inserted in Eq. (4.1) after removing the baseline and converting it in mm. Figure 4.10 illustrates the cavity voltage computed from the HT signals discussed in Section 4.2. Note that the x-axis here doesn't correspond to the 25 ns as previously but to the bunch length with $t = 0$ at zero crossing. The corresponding optic parameters are listed in Table 4.2

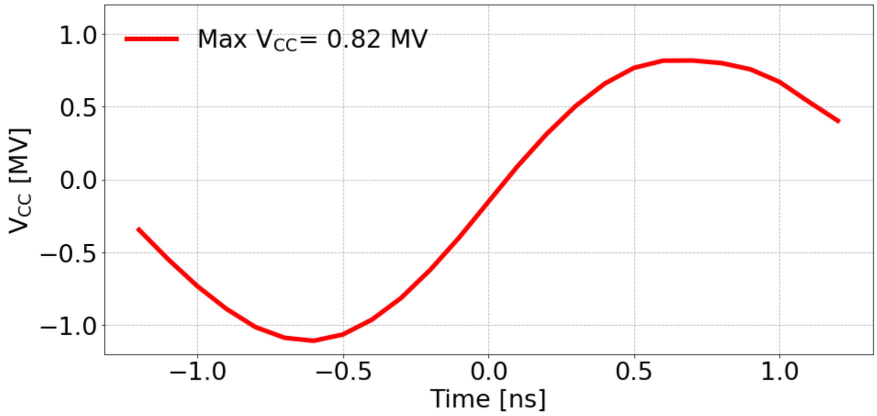

Figure 4.10: Intra-bunch offset from the CC kick expressed in mm after the removal of the baseline.

Table 4.2: Parameters for computing the CC voltage from the example HT monitor measurements discussed in this chapter

Parameters	**Units**	**Values**
$\beta_{y,HT}$ / $\beta_{y,CC1}$	[m]	49.19 / 76.07
$\psi_{y,HT}$ / $\psi_{y,CC1}$	[-]	15.68 / 23.9
Q_y	[-]	26.13
E_b	[GeV]	26

4.4 Reconstruction of crabbing

Physicall illustration of crabbing. Assuming gaussian transverse distribution. Approximation

Reconstruction of crabbing

4.5 Conclusions

Chapter 5

Emittance growth measurements with Crab Cavity noise in 2018

In 2018, two prototype Crab Cavities (CCs) were installed in the SPS to be tested for the first time with proton beams. One of the operational issues that needed to be addressed concerned the expected emittance growth due to noise in their RF control system. A theoretical model that describes this emittance growth had already been developed and validated by tracking simulations [1]. Based on those studies a dedicated experiment was performed to benchmark the models with experimental data and to confirm the analytical predictions. In particular, the idea was to inject various noise levels in the CC RF system and record the emittance evolution. In this chapter, the experimental procedure, the measurement methods and results are presented and discussed.

The chapter is stractured as follows: Section 4.1 describes the operational setup for the SPS CC tests and discusses the main diagnostic deployed for the derivation of the CC voltage.

blah blah ... describe sections and subsections after they are completed.

blah blah ... describe sections and subsections after they are completed.

blah blah ... describe sections and subsections after they are completed.

5.1 Crab Cavities in the SPS

For the SPS tests two prototype CCs of the Double Quorter Wave (DQW) type were fabricated by CERN and were assembled into the same cryomodule [2]. The cryomodule was installed in the SPS-LSS6 zone and was placed on a mobile transfer table [**GarlaschÃĺ:2648553**]. The table moved with high precision and without breaking the vaccum the cryomodule in the beam line for the CC tests and out of it for the usual SPS operation. For the emittance growth measurements only one of these CCs was used and its main optics and desgin parameters are listed in Table **??**.

5.2 Experimental procedure

5.2.1 Machine and beam configuration

5.2.2 Measurement methods

What do we measure and how? emittance (show plot ws) bunch length ABWLM –> we take the measurement directly from the resposnible tema –> show also from the instrument that we saw the unstable bunches.

5.3 Experimental resutls

5.3.1 Overview

- bunches 2, 3 and 4 unstable

5.3.2 Comparison with the theory

This chapter is adapted from the the studies published in Ref. [9]

5.4 Experimental Setup

Several experimental studies have been performed (2010-2017) to identify the optimal conditions for the emittance growth studies with CCs in the SPS [10, 11]. Based on these preparatory studies, the measurements in the SPS were performed with four low intensity ($\sim 3 \cdot 10^{10}$ ppb) bunches at 270 GeV. To minimise the emittance growth from other sources [11] the first order chromaticity, Q', of the machine was corrected to small positive values ($\sim$ 1-2) in both the horizontal and the vertical planes. During the measurements the Landau octupoles were switched off. It should be note, though, that a residual non-linearity was present in the machine mainly due to multipole components in the dipole magnets [12, 13]. Only one CC was used, providing a vertical kick to the beam. The transverse feedback system was switched off. Even though the emittance growth is a single bunch effect four bunches were used to reduce the statistical uncertainty of the measurements. The distance between the bunhces was 524 ns. An overview of the relevant SPS parameters during the experiment is given in Table

5.4.1 Injected RF noise

In order to characterize the CC noise induced emittance growth, controlled noise was injected into their LLRF system and the evolution of the bunch was recorded for about 20-40 minutes. The injected noise was a mixture of amplitude and phase noise up to 10 KHz, overlapping and primarily exciting the fisrt betatron sideband at ~ 8 kHz. The phase noise was always dominant.

Chapter 6

Investigation of the discrepancy

Chapter 7

Simple model of describing the decoherence suppression from impedance

Chapter 8

Application and impact for HL-LHC

Chapter 9

Conclusion

Appendix A

Appendix Title

Bibliography

[1] P. Baudrenghien and T. Mastoridis. "Transverse emittance growth due to rf noise in the high-luminosity LHC crab cavities". In: *Phys. Rev. ST Accel. Beams* 18 (10 Oct. 2015), p. 101001. DOI: 10.1103/PhysRevSTAB.18.101001. URL: https://link.aps.org/doi/10.1103/PhysRevSTAB.18.101001.

[2] C. Zanoni et al. "The crab cavities cryomodule for SPS test". In: 874 (July 2017), p. 012092. DOI: 10.1088/1742-6596/874/1/012092. URL: https://doi.org/10.1088/1742-6596/874/1/012092.

[3] Rama Calaga, Ofelia Capatina, and Giovanna Vandoni. "The SPS Tests of the HL-LHC Crab Cavities". In: (2018), TUPAF057. 4 p. DOI: 10.18429/JACoW-IPAC2018-TUPAF057. URL: https://cds.cern.ch/record/2649807.

[4] Carver Lee. *First proton beam dynamics results with crab cavities.* Accessed: 10-11-2021. URL: https://indico.cern.ch/event/800428/attachments/1804664/2945632/CrabCavity_BE_Seminar.pdf.

[5] Thomas Levens, Kacper Łasocha, and Thibaut Lefèvre. "Recent Developments for Instability Monitoring at the LHC". In: (2017), THAL02. 4 p. DOI: 10.18429/JACoW-IBIC2016-THAL02. URL: https://cds.cern.ch/record/2313358.

[6] R. Jones and H. Schmickler. "The measurement of Q' and Q" in the CERN-SPS by head-tail phase shift analysis". In: *PACS2001. Proceedings of the 2001 Particle Accelerator Conference (Cat. No.01CH37268).* Vol. 1. 2001, 531–533 vol.1. DOI: 10.1109/PAC.2001.987561.

[7] T. E. Levens et al. "Automatic detection of transverse beam instabilities in the Large Hadron Collider". In: *Phys. Rev. Accel. Beams* 22 (11 Nov. 2019), p. 112803.

DOI: 10.1103/PhysRevAccelBeams.22.112803. URL: https://link.aps.org/doi/10.1103/PhysRevAccelBeams.22.112803.

[8] Alexander Wu Chao et al. *Handbook of accelerator physics and engineering; 2nd ed.* Singapore: World Scientific, 2013. DOI: 10.1142/8543. URL: https://cds.cern.ch/record/1490001.

[9] Natalia Triantafylou. "INVESTIGATION OF DAMPING EFFECTS OF THE CRAB CAVITY NOISE INDUCED EMITTANCE GROWTH". In: (2021), TBA. DOI: TBA. URL: TBA.

[10] R Calaga et al. "Proton-beam emittance growth in SPS coasts". In: *Conf. Proc.* C1205201 (May 2012), THPPP007. 3 p. URL: https://cds.cern.ch/record/1451286.

[11] Fanouria Antoniou et al. "Emittance Growth in Coast in the SPS at CERN". In: *J. Phys.: Conf. Ser.* 1067 (2018), MOPMF061. 7 p. DOI: 10.18429/JACoW-IPAC2018-MOPMF061. URL: https://cds.cern.ch/record/2649815.

[12] Michele Carlà et al. "Studies of a New Optics With Intermediate Transition Energy as Alternative for High Intensity LHC Beams in the CERN SPS". In: (2018), TUPAF022. 4 p. DOI: 10.18429/JACoW-IPAC2018-TUPAF022. URL: https://cds.cern.ch/record/2664976.

[13] Androula Alekou et al. "SPS Long Term Stability Studies in the Presence of Crab Cavities and High Order Multipoles". In: (2018), WEP2PO008. 3 p. DOI: 10.18429/JACoW-HB2018-WEP2PO008. URL: https://cds.cern.ch/record/2640326.